

# Push Recovery for NAO Humanoid Robot

Payam Ghassemi

Human and Robot Interaction Lab.,  
Faculty of  
New Sciences and Technologies,  
University of Tehran, Tehran, Iran.  
Email: payam.ghassemi@ut.ac.ir

Mehdi Tale Masouleh

Human and Robot Interaction Lab.,  
Faculty of  
New Sciences and Technologies,  
University of Tehran, Tehran, Iran.  
Email: m.t.masouleh@ut.ac.ir

Ahmad Kalhor

Human and Robot Interaction Lab.,  
Faculty of  
New Sciences and Technologies,  
University of Tehran, Tehran, Iran.  
Email: akalhor@ut.ac.ir

**Abstract**—This paper presents the ankle, hip, and ankle-hip strategies in frontal plane for NAO humanoid robot. A humanoid is an unstable robotic mechanical system and the main and primary task of each humanoid is to maintain its balance. Moreover, NAO humanoid robot has 25 degrees-of-freedom with brushless DC actuators. The main challenges in the context of balancing of NAO humanoid are the high complexity of the robot and applying joint torque control approaches for NAO humanoid which is a position controlled robot. In this paper, for recovery and prediction the robot from external push, as the main contribution, the virtual leg model is proposed. The control objective is absorbing the external push and then recover the robot to its original configuration. PD controller is used to achieve the control objective. The performance and usage of these strategies and the model is validated by Webots. For each case study, an impulsive force is applied to NAO's torso with various magnitudes. The performance and validation of the proposed push recovery schemes are verified in the simulation. Moreover, the same results are obtained from the practical implementation of these strategies on NAO H25 humanoid robot.

**Index Terms**—Humanoid robot, Under-actuated system, Balance, and Push recovery

## I. INTRODUCTION

Humanoid and bipedal robots have a locomotion system like humans which make them suitable for most of human environments. A humanoid robot can be considered as a hybrid, tree-type multi-body mechanical system [1], [2]. Moreover, a humanoid robot is classified as a mobile robot for which one of the bodies shall be defined as a base body (float-base body). Obviously, humanoid robot has some additional Degrees-of-Freedom (DoF) due to the float-base body in which there are no direct actuators for affecting those DoF; i.e., humanoids can be regarded as under-actuated mechanical system.

Moreover, a humanoid robot is an unstable robotic mechanical system and the main and primary task of each humanoid is to maintain its balance. A humanoid robot is balanced until it is not fallen down which it can be provided by controlling the robot's interaction with its environment. The humanoid robots face with various disturbances due to the dynamic and unknown environment that is in interacting with it [2]. Moreover, in order to define a task, the full-body model of the robot with many uncertainties or some simplified models are used; although, tasks are defined in a way that humanoid is remained stable and balanced, the robot will fall. It is essential

to establish a push recovery control strategy to maintain humanoid balancing while there are various disturbances [3].

Balancing and push recovery are addressed in bio-mechanical researches for human cases and then are specially studied for humanoid robots. Ankle, hip, ankle-hip, and stepping strategies are the most known push recovery strategies of human [4]–[7]. The ankle strategy and hip strategy are introduced and studied in [6] in which it has been proposed that combining these two methods can be used for maintaining balance, ankle-hip strategy. In [4], it is found that human is using the ankle strategy and hip strategy based on an optimal effort criterion. The ankle, hip and ankle-hip strategies are described in more details in [5]. Moreover, in [5], some categories of various possible perturbations and differences of balancing strategies in stand and walking tasks are reviewed. In [7], the ankle and hip strategies are studied for a case when human is standing on a moving flat surface. One of the interesting results of the previous work is that by increasing the velocity of the standing surface, human employs the hip strategy with the ankle strategy and there is not a pure hip strategy. Ankle, hip and stepping strategies with multiple footsteps are studied in [8]. In addition, in [9], [10] the same strategies (with single footstep) are studied and a decision law is provided based on the position and velocity of CoM in order to decide to use each of those strategies for a given disturbance. For calculation of footstep various methods are introduced. In [2], capture points are defined for a single step strategy for push recovery. This index provides a capture region that robot can put its leg to fully stop. Then, Foot Placement Estimator (FPE) is introduced in [11] as a new measurement of balancing which are useful for generating dynamically balance gait cycles. An extension of the FPE, as called Foot Placement Indicator (FPI) is introduced in [12] to balance robot with stepping strategy. FPI takes into account the potential and kinetic energy of all links of the biped and the impulsive, discontinuous impact dynamics to determine proper foot placement [12]. Push Recovery Model Predictive Control (PR-MPC) introduced in [13] to balance a humanoid by stepping strategy with multiple footsteps. Recently, stepping strategy using a Linear Model Predictive Controller (LMPC) is developed in [14], [15] to maintain balance by producing a complete multiple footsteps. Moreover,



Fig. 1: NAO humanoid robot, H25 v4.

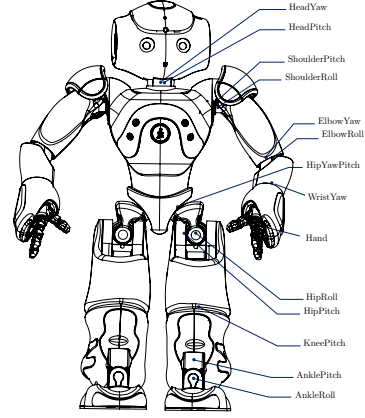


Fig. 2: Nao humanoid robot with 25-DoF.

the effects of upper-body motions for reducing the footstep lengths for push recovery are studied.

To balance a humanoid robot, the reaction of interaction with environment should be controlled. Based on this fact, some authors proposed several balancing schemes based on reaction forces control and optimization techniques. In [16], the balancing constraints, e.g. ZMP, CoM, reaction forces and etc., of a biped as a Second-Order Cone Programming (SOCP) programming are introduced which can be solved as a convex optimization problem. But this is not too practical due to huge computational costs. A momentum-based balance controller is proposed by [17] on a non-level and moving surface to maintain the desired ground reaction force and CoP at each support foot. A new balancing control law based on contact force optimization is proposed in [18]. This controller brings the ground reaction force to a desired value that insure robot will be balanced.

In real robots, e.g., Honda humanoid robots [19], a combination of the various methods are used and the simple strategies are still the most popular methods; the ankle, hip, ankle-hip and stepping strategies not only used by humans but also are computationally cost effective. In this paper, the ankle, hip, and ankle-hip strategies in frontal plane are implemented on NAO humanoid robot (Figure 1) which is a position controlled robot. The remainder of this paper is organized as follows.

First, NAO humanoid robot is introduced and the kinematics and dynamic model in 3D are provided in Section II. In Section III, the balancing strategies are described and the simplified model for each case are introduced. Finally, the balancing strategies are simulated on a NAO humanoid model which provided by Webots and the results are given in Sections IV and V.

## II. THE NAO HUMANOID ROBOT

NAO is a Humanoid robot developed by Aldebaran Robotics and RoboCup competition included NAO Standard Platform League since 2008. Aldebaran Robotics has provided various version of robots in various categories. The most advanced version of this robot is NAO H25 v4, as shown in Fig. 1, which has some significant improvement rather than previous models.

NAO H25 is known as academic version with 25 Degree-of-Freedoms (Fig. 2).

### A. Dynamic Model

As mentioned before, a humanoid robot is a float-based mechanical system with a mandatory interaction with environment. The dynamic model of a humanoid in a complete form can be obtained by using the Lagrangian method and defining the generalized coordinates as follows:

$$\mathbf{x} = [\mathbf{x}_{b,p}^T, \mathbf{x}_{b,r}^T, q_1, \dots, q_{25}]^T, \quad (1)$$

where  $\mathbf{x}_{b,p}$  and  $\mathbf{x}_{b,r}$  represent the position and the orientation of the float-base body, respectively. Also,  $q_i$  corresponds to the angle of the  $i$ -th joint of robot. Then, the dynamic model of humanoid robot can be written in the following form:

$$\begin{bmatrix} \mathbf{M}_b & \mathbf{M}_{br} \\ \mathbf{M}_{br}^T & \mathbf{M}_r \end{bmatrix} \begin{bmatrix} \dot{\mathbf{v}}_b \\ \dot{\mathbf{q}}_r \end{bmatrix} + \mathbf{c}(\mathbf{x}, \dot{\mathbf{x}}) + \mathbf{g}(\mathbf{x}) = \begin{bmatrix} \mathbf{0} \\ \boldsymbol{\tau} \end{bmatrix} + \sum_{i=1}^r \mathbf{J}_i^T \mathbf{f}_i \quad (2)$$

where,  $\mathbf{M}_{bb}$  represents to the inertia felt at the base,  $\mathbf{M}_{rr}$  represents the joint space inertia of the robot, and  $\mathbf{M}_{br}$  corresponds to the inertial weight between accelerations of the base and the resulting torques on the actuated joints, as indicated in [20]. It should be mentioned that  $\mathbf{M}_{bb}$ ,  $\mathbf{M}_{br}$ , and  $\mathbf{M}_{rr}$  are independent on the global position and orientation of the robot [20]. The parameters  $\mathbf{f}_i$ ,  $\mathbf{J}_i$  represent the constrained forces, e.g. ground reaction forces and the corresponded Jacobian matrix, respectively. Finally,  $\mathbf{c}$  and  $\mathbf{g}$  correspond to the centrifugal and Coriolis forces and the gravitational forces, respectively.

### B. Planar Models

The three dimensional model of a robot is useful for simulation and some tasks that need the entire dynamics and inertial properties of robot to get involved with significant velocities and accelerations. Planar models and simplified models are proposed as some appropriate control models based on the design of most real humanoids and common tasks, for example: walking, running, sitting, picking up loads and objects and so on. Three planes are defined for human and humanoid robots [21]:

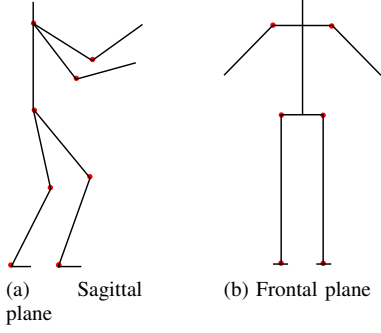


Fig. 3: The planar model for NAO humanoid.

- 1) Sagittal plane: the plane that divides the body into right and left sides.
- 2) Frontal plane: the plane that separates the body into front and back sections.
- 3) Transverse plane: the plane that is perpendicular to both the sagittal and frontal planes.

Based on the specifications and design of NAO, two planar models, one in the sagittal plane and another one in the frontal plane, are obtained as shown in Fig. 3. For both models, only the DoF are chosen which have significant effects in the balancing of NAO if the full-body model in each plane is considered. Thus, NAO will have 10-DoF and 6-DoF in the sagittal plane and the frontal plane, respectively. These models are useful for balancing methods based on full-body model which will be addressed in the future works.

In this paper, the push recovery in the frontal plane based on the ankle, hip and ankle-hip strategies are investigated. Thus, a more simplified model, as the main contribution of this paper, is proposed for these strategies in this paper, which is called virtual leg model (Figure 4). In this paper, the virtual leg is defined by attaching a virtual link between two virtual revolute joints as placed exactly between the left and right hip joints and left and right ankle joints in the frontal plane<sup>1</sup> and the upper-body is modeled as a single link. The joints of the virtual leg are related to the hip and ankle joints of both legs as follows:

$$\theta_{rh} = \theta_{vh}, \quad \theta_{lh} = \theta_{vh}, \quad \theta_{ra} = \theta_{va}, \quad \theta_{la} = \theta_{va}. \quad (3)$$

where “r”, “l”, “h”, and “a” indices stand for “right”, “left”, “hip”, and “ankle”, respectively.

The equation of motion of the virtual leg model is obtained using the Lagrangian method. The kinetic energy  $\mathcal{K}$  and the potential energy  $\mathcal{P}$  are written as follows:

$$\mathcal{K} = \frac{1}{2}(m_1 + m_2)l_1^2\dot{\theta}_1^2 + \frac{1}{2}m_2l_2^2\dot{\theta}_2^2 + m_2l_1l_2\dot{\theta}_1\dot{\theta}_2 \cos(\theta_2 - \theta_1) \quad (4)$$

$$\mathcal{P} = -(m_1 + m_2)gl_1 \cos \theta_1 - m_2gl_2 \cos \theta_2 \quad (5)$$

where  $m_1$ ,  $m_2$ ,  $l_1$ , and  $l_2$  are the equivalent mass and length of each virtual link, respectively. Then, the Lagrangian  $\mathcal{L}$  is

<sup>1</sup>These joints are corresponded to “LHipRoll”, “RHipRoll”, “LAnkleRoll” and “RAnkleRoll” joints as

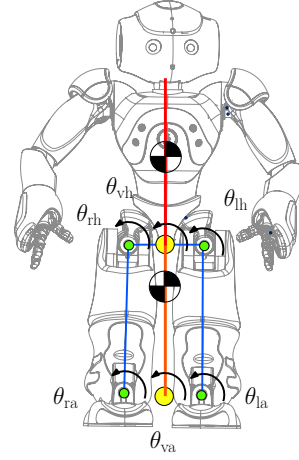


Fig. 4: The virtual leg model.

obtained as:

$$\mathcal{L} = \mathcal{K} - \mathcal{P} \quad (6)$$

and the Lagrange equation is

$$\frac{d}{dt} \left( \frac{\partial \mathcal{L}}{\partial \dot{\theta}_i} \right) - \frac{\partial \mathcal{L}}{\partial \theta_i} = \tau_i, \quad i = 1, 2. \quad (7)$$

Thus, the motion equations of the virtual leg model is given as follows:

$$\mathbf{M}(\boldsymbol{\theta})\ddot{\boldsymbol{\theta}} + \mathbf{c}(\boldsymbol{\theta}, \dot{\boldsymbol{\theta}}) + \mathbf{g}(\boldsymbol{\theta}) = \boldsymbol{\tau} \quad (8)$$

where

$$\mathbf{M} = \begin{bmatrix} (m_1 + m_2)l_1^2 & m_2l_1l_2 \cos(\theta_2 - \theta_1) \\ m_2l_1l_2 \cos(\theta_2 - \theta_1) & m_2l_2^2 \end{bmatrix} \quad (9)$$

$$\mathbf{c} = \begin{bmatrix} -m_2l_1l_2\dot{\theta}_2^2 \sin(\theta_2 - \theta_1) \\ m_2l_1l_2\dot{\theta}_1^2 \sin(\theta_2 - \theta_1) \end{bmatrix} \quad (10)$$

$$\mathbf{g} = \begin{bmatrix} (m_1 + m_2)gl_1 \sin \theta_1 \\ m_2gl_2 \sin \theta_2 \end{bmatrix} \quad (11)$$

$$\boldsymbol{\theta} = [\theta_1 \quad \theta_2]^T \quad (12)$$

$$\boldsymbol{\tau} = [\tau_1 \quad \tau_2]^T \quad (13)$$

### III. PUSH RECOVERY

Maintaining the balance of a robot while an external disturbance applied to it, is an essential ability for a humanoid to be able to work in real environment. Thus, the control objective is defined as: keeping the posture of robot in upright while external forces are applied to any part of robot.

#### A. Push Recovery Strategies

The selected strategies for this objective are the human-inspired ones:

- 1) Ankle strategy: The robot posture is maintaining upright using the ankle joints. The motion of the ankle joints are limited and if a torque with more than an allowable value is applied then the contact between robot foot and ground will be lost. Thus, it is a restricted ability to push recovery and reject the disturbance of robot.

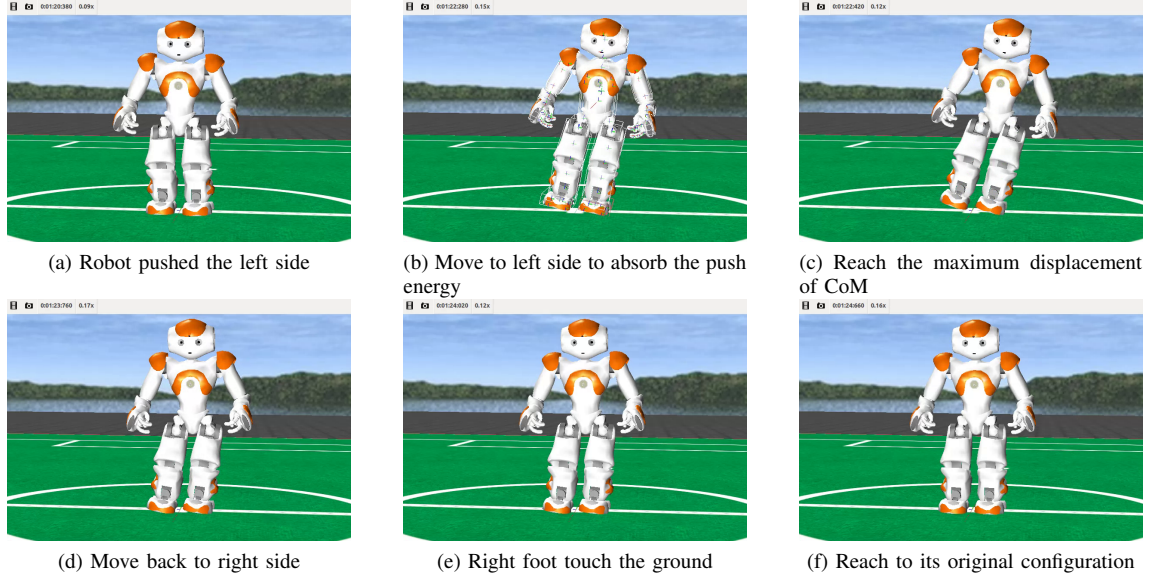


Fig. 5: Snapshots of the hip strategy to push recovery in Webots for NAO (the maximum displacement of CoM is depended on the magnitude of the external push based on stiffness and damping coefficients).

- 2) Hip strategy: The robot posture keeps the robot upright using the hip joints. This strategy changes the upper-body position and orientation and it is not required to change the lower-body motions. Thus, the hip strategy is more appropriate for balancing of humanoid while doing the other tasks like walking.
- 3) Ankle-hip strategy: The robot uses a combination of the above strategies to push recovery. It eliminates the problem that can be raised in the hip strategy; when a disturbance brings robot to unstable situations and the feet are tipped over, the ankle-hip strategy keeps the contact of feet more reliable than the hip strategy.

It worth to be mentioned that, for each specific task and disturbance magnitude one of those strategies could be more appropriate and effective. In order to apply these strategies simultaneously in an appropriate way, a decision making policy is essential. However, this decision policy is beyond of the scope of this work and will be published in an upcoming publication.

### B. Control Law

As described in Section II, a virtual leg model is proposed for applying the above strategies; i.e., the control inputs and system states for each strategy as described in Table I. For maintaining the balance, the steady error is not too important and moreover the integral term decreases the quality of transient response and the stability. Thus, to calculate the control input, PD-controller is used; i.e.,

$$u = K_P(x_d - x_a) + K_D(\dot{x}_d - \dot{x}_a) \quad (14)$$

where  $K_P$ , and  $K_D$  are the proportional gain and the derivative gain constants. For each strategy, the coefficients of PD controller are provided in Table I. The gains of each controller

are optimized in a manual way that under the same disturbance force, the controller provides a smooth response for the CoP trajectory.

## IV. SIMULATION

To evaluate the balancing strategies and their corresponding control law for NAO humanoid, they are implemented in a simulation environment. Hence, it is possible to verify them without any possible dangers of robot damaging and with most freedom to apply various scenarios. The pseudo-code for the push recovery is shown in 1.

### A. Simulation Environment

To minimize the time of converting the same implemented control methods from a simulated robot to real one, a specific release of the simulator software Webots <sup>72</sup> [22] is used. The software provide a complete model of NAO with the same sensors, actuators and specifications. Moreover, the same codes that are valid to be run on a NAO humanoid model in this software, can be applied to a real NAO humanoid robot without any modifications.

Since the C++ framework is the most complete framework for NAO and the only one that can provide real-time implementation [22], all codes are implemented in C/C++ language. The codes are written based on the official C++ SDK "naoqi-sdk-1.14.3-linux32" which is provided by Aldebaran Robotics.

### B. Simulation Settings

For each case study, an impulsive force is applied to NAO's torso with various magnitudes. Unfortunately, in this version of software it is not possible to exactly control the applied force and the duration of each disturbance. Thus, using the trial

<sup>72</sup>Webots for NAO.

TABLE I: The virtual leg and PD control parameters for the strategies.

	System state(s)	Control input(s)	The gains of PD controller		Maximum force [N]
			$K_P$	$K_D$	
Ankle strategy	$\theta_{va}, \dot{\theta}_{va}$	$\tau_{va}$	0.50	0.01	$\sim 100$
Hip strategy	$\theta_{vh}, \dot{\theta}_{vh}$	$\tau_{vh}$	1.20	0.1	$\sim 140$
Ankle-hip strategy	$\theta_{va}, \dot{\theta}_{va}, \theta_{vh}, \dot{\theta}_{vh}$	$\tau_{va}, \tau_{vh}$	{0.80, 1.00}	{0.02, 0.25}	$\sim 130$

**Algorithm 1:** Push recovery psuedo-code for the lateral disturbance.

---

**Input:**  $q_{reference}, \dot{q}_{reference}$ , and  $\theta_{base}$   
**Output:**  $q_{controlRobot}$   
**while**  $\theta_{base} \neq \epsilon$  **do**  
     $q_{actual} \leftarrow \text{VirtualLeg}(\theta_{robot});$   
     $e \leftarrow q_{reference} - q_{actual};$   
     $\dot{e} \leftarrow \dot{q}_{reference} - \dot{q}_{actual};$   
     $\tau \leftarrow \text{PDCotroller}(e, \dot{e});$   
     $q_{control} \leftarrow \text{VirtualDynamicModel}(\tau)$   
     $q_{controlRobot} \leftarrow \text{InverseVirtualLeg}(q_{control});$   
**end**

---

and error tests the approximately maximum force is obtained for each case which is applied just for a single simulation step. The position and orientation of the robot are observed in the world space framework. The loop control cannot be higher than 10 ms due to the delay of access to the sensor information. Hence, each loop takes about 11-23 ms time in the current implementation of the code.

## V. RESULTS AND DISCUSSION

The performance and validation of the proposed push recovery schemes are evaluated in the simulation, as described in Section IV. Successful push recovery strategies were verified for disturbances in the frontal plane. The simulation results for various disturbances and different strategies are shown in Figs. 6-8. Approximately maximum disturbance force for each strategy, which applied to the torso of robot is summarized in Table I. Figure 5 depicts some snapshots for an arbitrary push recovery using the hip strategy in the frontal plane.

The center of pressure for each strategy is represented in Figs. 6a,7a, and 8a and the center of mass displacements are shown in Figs. 6b, 7b, and 8b. As it can be observed from the later figures, the center of pressure in each case is successfully brought to initial state and there is only an offset in the ankle-hip strategy. Moreover, the displacement of the center of mass is successfully recovered and the hip strategy has the best response. The main reason for this offset and error on the ankle-hip strategy is due to the fact that each controller provide control input for each joint individually. Thus, by considering the virtual leg model as a Multi-Input-Multi-output (MIMO) system to improve the ankle-hip strategy. In addition, the inclination of base of virtual leg model should be evaluated using an accurate way which can correctly consider both angles.

The results reveal that the hip and ankle-hip strategies are more appropriate for larger disturbances, as it was expected. Moreover, as it can be inferred from from Figs. 6b, 7b, and 8b, the hip strategy brings robot to its balance configuration in more smooth way and adding the hip strategy to the ankle strategy provides more smooth and fast balancing in comparison to each single strategy. There is a steady-state error for all cases. Furthermore, the results of the practical implementation verify the proposed approaches. The same strategies were successfully implemented for the frontal disturbances while their results were not represented in this work due to the page limitation.

## VI. CONCLUSION

Push recovery of NAO humanoid robot was provided based on the ankle, hip, and ankle-hip strategies. These strategies were implemented in C++ language and verified in Webots software which provides one of the best simulated model of real NAO. The results verified the performance and practical effectiveness of these strategies for NAO humanoid H25 in standing cases. In addition, some preliminary practical implementations on real NAO humanoid verified the simulated results. Providing the stepping strategy for the frontal plane are considered as ongoing works.

## REFERENCES

- [1] Y. Hurmuzlu, F. Gnot, and B. Brogliato, "Modeling, Stability And Control Of Biped Robots - a General Framework," *Automatica*, vol. 40, no. 10, p. 16471664, 2004.
- [2] J. Pratt, J. Carff, S. Drakunov, and A. Goswami, "Capture Point: A Step Toward Humanoid Push Recovery," in *6th IEEE-RAS International Conference on Humanoid Robots*. IEEE, 2006, p. 200207.
- [3] S.-k. Yun and A. Goswami, "Momentum-based reactive stepping controller on level and non-level ground for humanoid robot push recovery," in *IEEE/RSJ International Conference on Intelligent Robots and Systems (IROS)*. IEEE, 2011, p. 39433950.
- [4] A. D. Kuo, "An optimal control model for analyzing human postural balance," *IEEE Transactions on Biomedical Engineering*, vol. 42, no. 1, p. 87101, 1995.
- [5] D. A. Winter, "Human Balance And Posture Control During Standing And Walking," *Gait & posture*, vol. 3, no. 4, p. 193214, 1995.
- [6] F. B. Horak, L. M. Nashner *et al.*, "Central programming of postural movements: Adaptation to altered support-surface configurations," *J Neurophysiol*, vol. 55, no. 6, pp. 1369-1381, 1986.
- [7] C. Runge, C. Shupert, F. Horak, and F. Zajac, "Ankle and hip postural strategies defined by joint torques," *Gait & Posture*, vol. 10, no. 2, pp. 161-170, 1999.
- [8] K. Yin and M. van de Panne, "Omnidirectional humanoid balance control: Multiple strategies for reacting to a push," *Computer Science technical report TR-2006-11*, University of British Columbia, 2006.
- [9] B. Stephens, "Integral control of humanoid balance," in *IEEE/RSJ International Conference on Intelligent Robots and Systems (IROS)*. IEEE, 2007, pp. 4020-4027.
- [10] B. Stephens, "Humanoid push recovery," in *7th IEEE-RAS International Conference on Humanoid Robots*. IEEE, 2007, pp. 589-595.

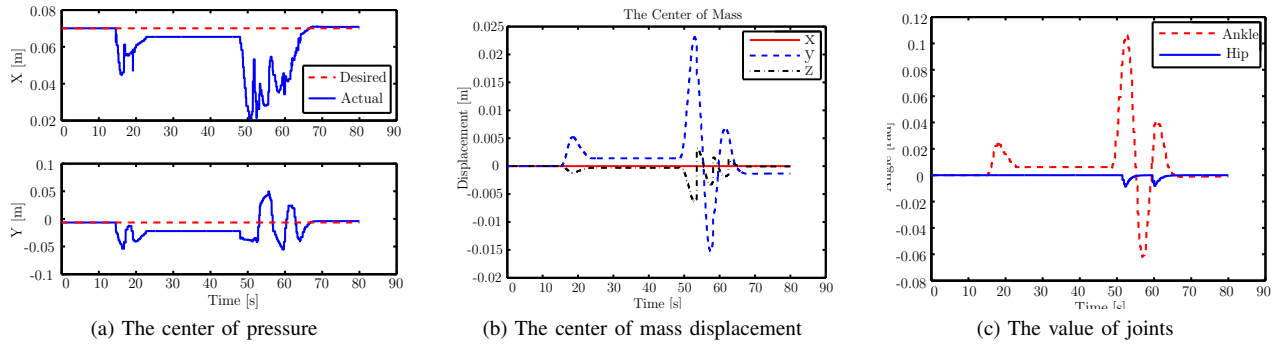


Fig. 6: The ankle strategy outputs in the frontal plane.

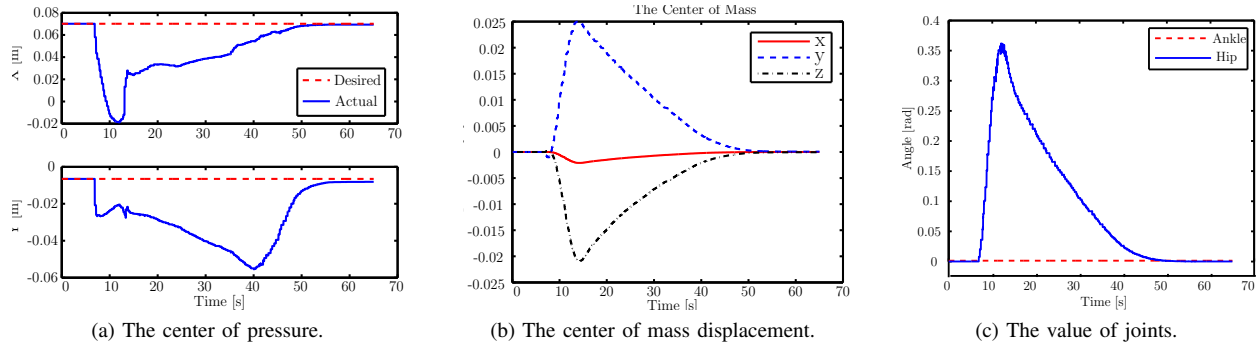


Fig. 7: The hip strategy outputs in the frontal plane.

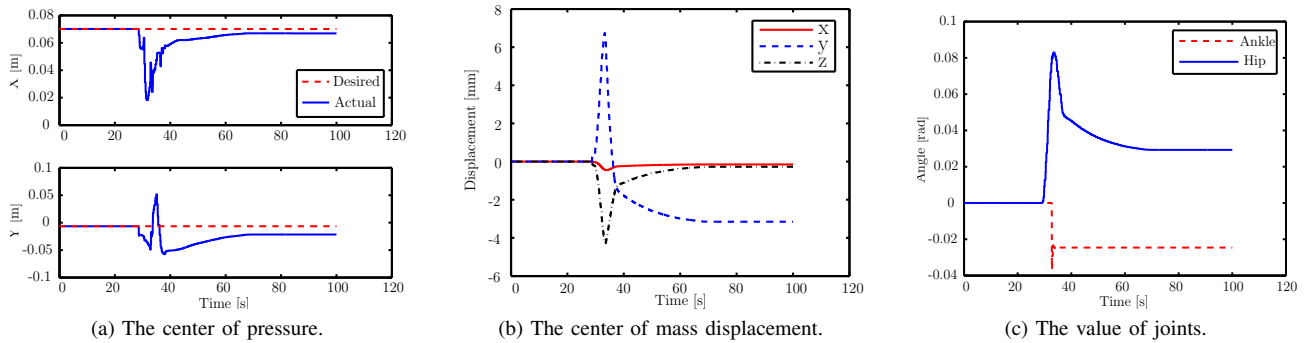


Fig. 8: The ankle-hip strategy outputs in the frontal plane.

- [11] D. L. Wight, E. G. Kubica, and D. W. Wang, "Introduction of the foot placement estimator: A dynamic measure of balance for bipedal robotics," *Journal of computational and nonlinear dynamics*, vol. 3, no. 1, p. 011009, 2008.
- [12] P. van Zutven and H. Nijmeijer, "Balance of humanoid robots by proper foot placement," in *Proceedings of the Dynamic Walking Conference*, 2012.
- [13] B. J. Stephens and C. G. Atkeson, "Push recovery by stepping for humanoid robots with force controlled joints," in *10th IEEE-RAS International Conference on Humanoid Robots (Humanoids)*. IEEE, 2010, p. 5259.
- [14] Z. Aftab, T. Robert, and P.-B. Wieber, "Predicting multiple step placements for human balance recovery tasks," *Journal of biomechanics*, vol. 45, no. 16, pp. 2804–2809, 2012.
- [15] Z. Aftab, T. Robert, and P.-B. Wieber, "Simulating the effect of upper-body inertia on human balance recovery," *Computer methods in biomechanics and biomedical engineering*, vol. 15, no. sup1, pp. 148–150, 2012.
- [16] J. Park, J. Haan, and F. C. Park, "Convex optimization algorithms for active balancing of
- vol. 23, no. 4, pp. 817–822, 2007.
- [17] S.-H. Lee and A. Goswami, "Ground reaction force control at each foot: A momentum-based humanoid balance controller for non-level and non-stationary ground," in *IEEE/RSJ International Conference on Intelligent Robots and Systems (IROS)*. IEEE, 2010, pp. 3157–3162.
- [18] C. Ott, M. A. Roa, and G. Hirzinger, "Posture and balance control for biped robots based on contact force optimization," in *11th IEEE-RAS International Conference on Humanoid Robots (Humanoids)*. IEEE, 2011, pp. 26–33.
- [19] T. Takenaka, "The control system for the honda humanoid robot," *Age and ageing*, vol. 35, no. suppl 2, pp. ii24–ii26, 2006.
- [20] L. Sentis, "Synthesis and control of whole-body behaviors in humanoid systems," Ph.D. dissertation, Citeseer, 2007.
- [21] E. R. Westervelt, J. W. Grizzle, C. Chevallereau, J. H. Choi, and B. Morris, *Feedback Control Of Dynamic Bipedal Robot Locomotion*. CRC press Boca Raton, 2007.
- [22] A. Robotics. (2014) Nao software documentation. [Online]. Available: <https://community.aldebaran-robotics.com/doc/1-14/>